This is an *Accepted Manuscript*, which has been through the Royal Society of Chemistry peer review process and has been accepted for publication.

Accepted Manuscripts are published online shortly after acceptance, before technical editing, formatting and proof reading. Using this free service, authors can make their results available to the community, in citable form, before we publish the edited article. We will replace this *Accepted Manuscript* with the edited and formatted *Advance Article* as soon as it is available.

You can find more information about *Accepted Manuscripts* in the **Information for Authors**.

Organic & Biomolecular Chemistry

RSC**Publishing**

Investigation of Transannular Cycloaddition Reactions involving Furanoxonium Ions using DFT Calculations. Implications for the Origin of Plumarellide and Rameswaralide and related Polycyclic Metabolites isolated from Corals.

B. Lygo,*[a] M. J. Palframan[a] and G. Pattenden*[a]

DFT calculations probing potential (4+2) and (4+3) cycloaddition pathways leading to the polycyclic ring systems found in the coral secondary metabolites plumarellide, mandapamate and rameswaralide are described. Formation of plumarellide and mandapamate via stepwise intramolecular cycloaddition of a furanoxonium ion onto a 1,3-diene is shown to be viable. The calculations also predict the outcome of related cyclisations involving model systems.
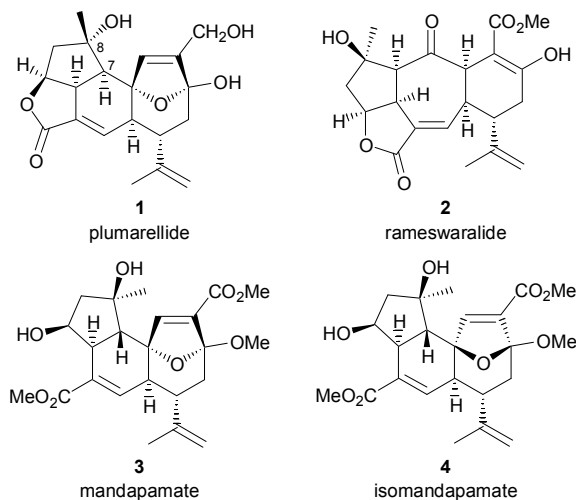
Introduction

Figure 1. Novel polycyclic structures found in corals

Plumarellide **1**, rameswaralide **2**, and the mandapamates **3** and **4** are novel polycyclic secondary metabolites which are believed to share a common biosynthetic origin. The metabolites **1**, **3** and **4** have a central cyclohexene ring in their structures, whilst ramseswaralide **2** instead has a cycloheptene ring as a key feature of its structure. The compounds also display subtle variations in stereochemistry at their C7 and C8 centres. Thus, the tertiary OH groups at C8 in **2**, **3** and **4** are orientated β, whereas the same OH group in plumarellide **1** has the corresponding α-orientation. Furthermore, the H-centre at
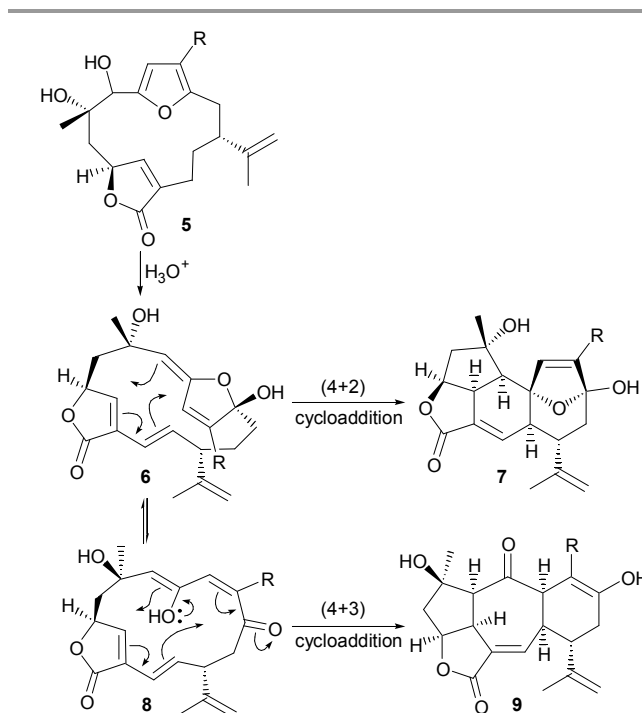

Scheme 1. Proposed biosynthesis of the ring systems **7** and **9** in plumarellide and rameswaralide respectively.

C7 in the metabolites **1** and **2** is on the α-face of their structures, but the same H-centre in the mandapamates **3** and **4** is on the opposite β-face of their structures.
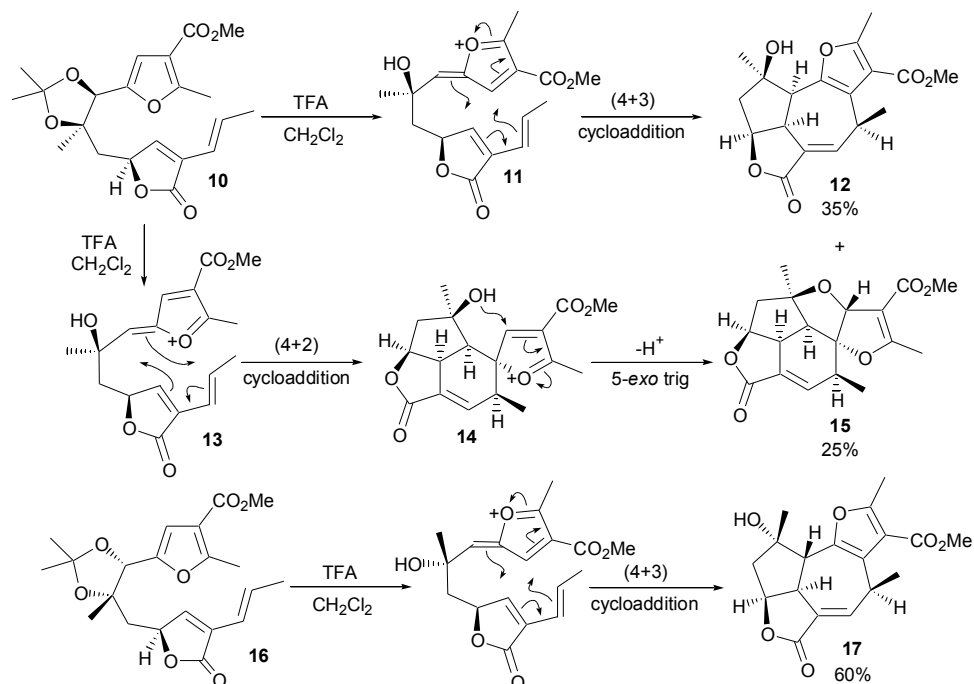
Scheme 2. Formation of the polycycles **12**, **15** and **17** via acid-catalysed rearrangement of the acetonides **10** and **16**.
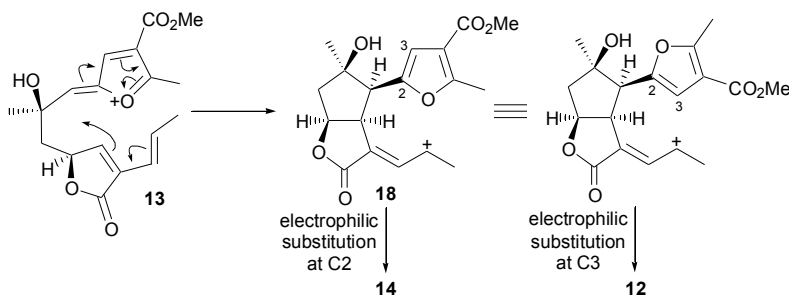

Scheme 3. Stepwise cyclisation pathways to **12** and **14** from the common furanoxonium ion intermediate **13**.

In earlier publications we have speculated that the metabolites **1-4** have their origins in furanobutenolide–based cembranoids, i.e. **5**, by way of elaboration to novel enol ether intermediates, e.g. **6**, followed by transannular (4+2) or (4+3) type cycloaddition reactions, viz. **6**→**7** and **8**→**9** (Scheme 1).[1] Indeed, during investigations of these proposals we showed that when the model furanobutenolide **10**, having an α-orientated oxy centre at C8 was treated with TFA in CH$_2$Cl$_2$ it underwent hydrolysis to the isomeric furanoxonium ion intermediates **11** and **13** which then underwent transannular cyclisation reactions leading to the polycycles **12** and **15** respectively in a combined overall yield of 60% (Scheme 2).[2] Interestingly, treatment of the diastereoisomeric acetonide **16** having a β-orientated oxy centre at C8 with TFA under the same conditions, gave only the cycloheptene ring-containing polycycle **17** and no corresponding cyclohexene ring-containing compound similar to **15**.[3]

Although we have represented the cyclisations leading to **12** and **15** taking place by (4+3) and (4+2) type cyclisations, via the isomeric furanoxonium ion intermediates **11** and **13** respectively, we have also suggested that the same overall conversions could be depicted as stepwise carbonium ion cyclisation processes, with the allylic carbonium ion **18** as the key intermediate (see Scheme 3).[2]
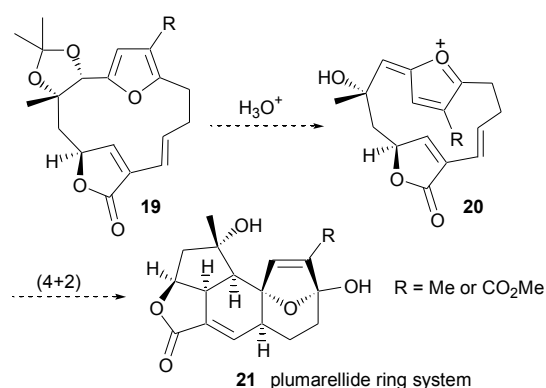
Scheme 4. A proposed pathway from the macrocycle **19** to the plumarellide ring system **21**.

Organic & Biomolecular Chemistry
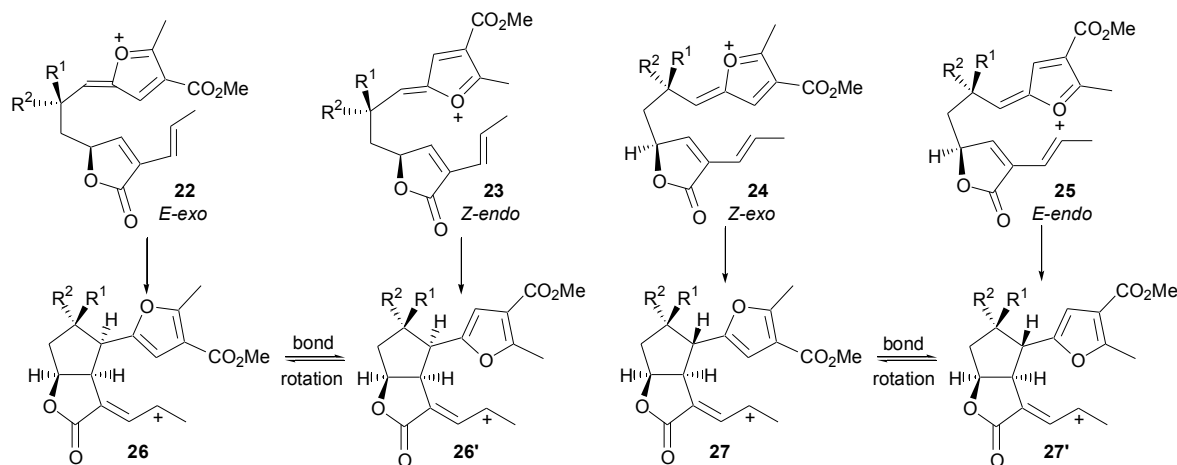
Scheme 5. Potential cyclisation pathways for furanoxonium ion intermediates derived from acetonides **10** and **16**.

In order to gain a more thorough appreciation of the likely reaction pathway, i.e. concerted or stepwise, followed by the furanoxonium ions **11** and **13** during their transannular cyclisations to **12** and **14** respectively, we have carried out DFT calculations[4] on these systems and also on the macrocyclic analogue **20** of **11/13** (produced from **19**, Scheme 4), which is more closely related to the proposed precursor **6** for the biosynthesis of natural plumarellide **1**.

Results and discussion

The aim of this study was to probe the intrinsic reactivity of the furanoxonium ions **11**, **13** and **20**, and related structures, and particularly their predisposition towards the different cyclisation pathways rather than to attempt to reproduce the experimental results *in silico*. For this reason we opted to employ gas phase (vacuum) calculations without applying any form of solvent correction.[5]

Initially B3LYP/6-31G(d)[6] was used to search for both stepwise and concerted cyclisation pathways corresponding to the transformations **11→12**, **13→14**, **16→17**. Geometric counterpoise (gCP) and dispersion (D3) corrections were applied to all of the structures generated in this way, as recommended by Grimme.[7] All of the structures were also re-optimised using B3LYP/6-31+G(d,p). This method has been widely utilised for DFT-based geometry optimisation in the study of biosynthetic pathways involving carbocation intermediates, and generally performs well when benchmarked against other methodologies.[8]

In each case we were only able to locate low energy transition states corresponding to stepwise cyclisation pathways in the three conversions **11→12**, **13→14** and **16→17** (*cf.* Scheme 3). This observation is consistent with two recent complementary studies of *intermolecular* (4+3) cycloadditions between substituted furanoxonium ions and 1,3-dienes which concluded that these also probably proceed *via* stepwise pathways.[9,10] The (4+3) cycloaddition of chiral alkoxysiloxy cations with furan has also been investigated using DFT calculations.[11] This study also concluded that the cycloaddition was most likely stepwise.

In each of the conversions **10** into **12** and **16** into **17** (Scheme 2) there are two possible isomeric furanoxonium ion

intermediates that could be generated, *i.e.* **22** and **23** from **10**, and **24** and **25** from **16** (Scheme 5). In the first step of the cyclisations of these furanoxonium ions, each could cyclise to their corresponding allylic carbonium ion intermediates **26** and **27**. In each case cyclisation could occur with the furanoxonium O-atom orientated either *exo-* or *endo-* relative to the diene, leading to the four viable stepwise cyclisation pathways shown in Scheme 5.[12] These cyclisations result in the production of two diastereoisomeric carbocation intermediates, *i.e.* **26/26'** and **27/27'** respectively.

Table 1. Relative Transition State Energies for the Cyclisation Modes Depicted in Scheme 5 (R^1=Me, R^2=OH, i.e. C8 α-hydroxy series).

Method[a]	Relative Energy (kcal/mol)[b]			
	E-exo	*Z-endo*	*Z-exo*	*E-endo*
B3LYP-gCP-D3/6-31G(d)	5.9	3.8	0	0.3
B3LYP/6-31+G(d,p)	4.8	2.8	0	1.0
BMK/6-311+G(d,p)//B3LYP/6-31+G(d,p)	3.9	2.2	0.4	0
M06-2X/6-31+G(d,p)	4.4	3.3	0	0.1

[a]For further details see supplementary data. [b]Based on Gibbs free energy values.

Table 2. Relative Transition State Energies for the Cyclisation Modes Depicted in Scheme 5 (R^1=OH, R^2=Me, i.e. C8 β-hydroxy series).

| Method[a]	Relative Energy (kcal/mol)[b]			
	E-exo	*Z-endo*	*Z-exo*	*E-endo*
B3LYP-gCP-D3/6-31G(d)	0	2.9	4.6	6.1
B3LYP/6-31+G(d,p)	0	1.8	1.8	3.7
BMK/6-311+G(d,p)//B3LYP/6-31+G(d,p)	0	2.3	3.4	5.6
M06-2X/6-31+G(d,p)	0	2.0	5.3	7.3

[a]For further details see supplementary data. [b]Based on Gibbs free energy values.

Predicted relative energies for the transition states of these cyclisation processes are given in Table 1 (for the C8 α-OH series, *i.e.* from **10**) and Table 2 (for the C8 β-OH series, *i.e.* from **16**). We have used the relative energy of the transition states here rather than comparing activation energies because larger errors in the latter would be expected due to the high number of degrees of freedom in the starting furanoxonium ions. IRC calculations[13] on the transition states led to 'starting

geometries' that were typically 8-14 kcal/mol lower in energy, providing an estimate of the minimum barrier to cyclisation. In addition to the methods described above, we also performed BMK/6-311+G(d,p)[14] single point calculations on B3LYP/6-31+G(d,p) optimised geometries and re-optimised the structures using M06-2X/6-31+G(d,p).[15] BMK/6-311+G(d,p)//B3LYP/6-31+G(d,p) was included as this has previously been shown to give good qualitative agreement with experiment when applied

to the intermolecular (4+3) cycloadditions of substituted furanoxonium ions to 1,3-dienes.[9] M06-2X/6-31+G(d,p) was included for comparison as this has been widely used in the study of reaction pathways in recent years and would be expected to superior when accounting for weak π-interactions.[16]
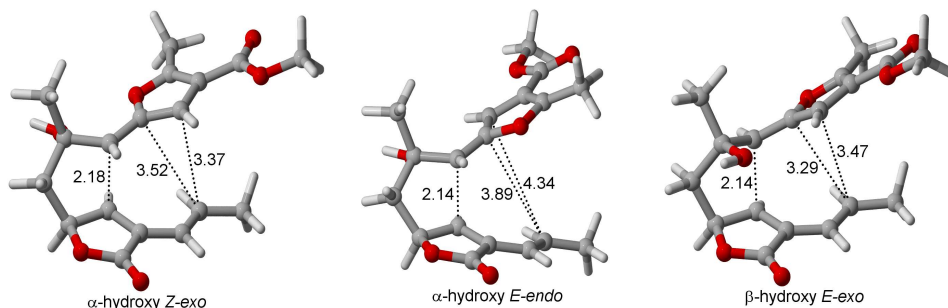
Figure 2. Favoured transition state structures for cyclisations of furanoxonium ion intermediates derived from the acetonides **10** and **16**. Atom distances are in Å.
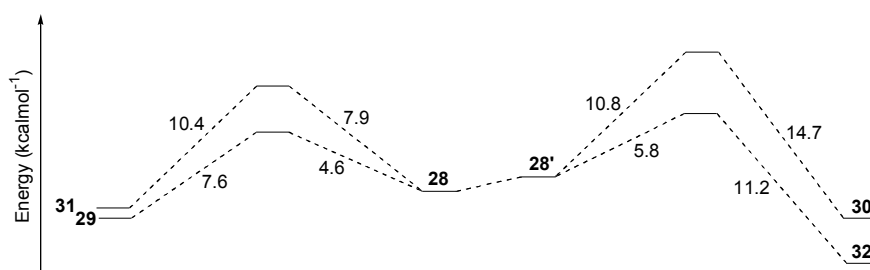
Figure 3. Free energy profile for the cyclisation pathways depicted in Scheme 6.
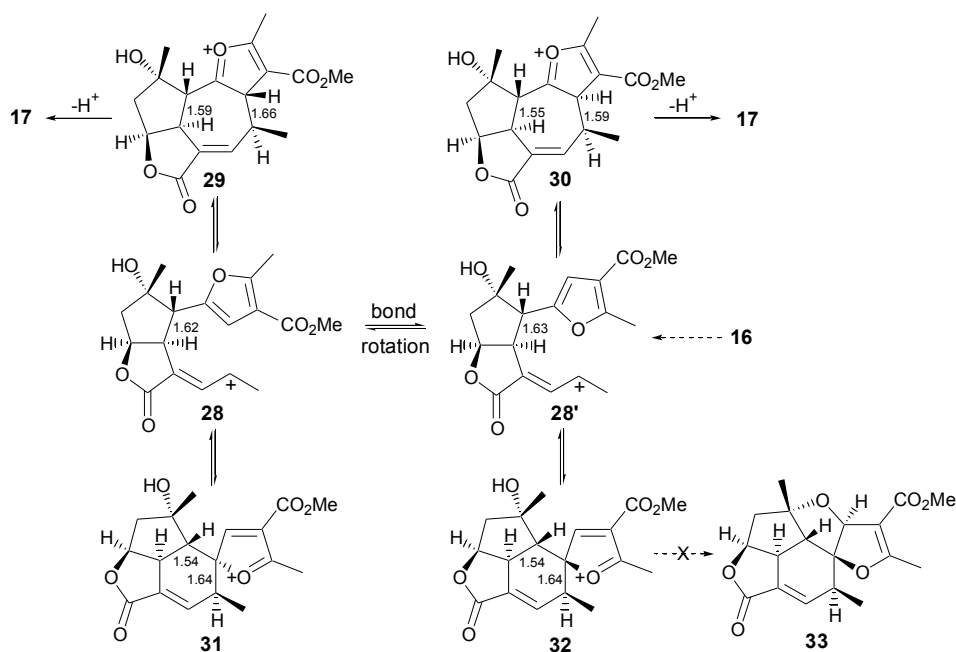
Scheme 6. Cyclisation pathways leading from the allylic carbocation intermediate **28**. Bond lengths (Å) shown are for the new bonds formed.

Figure 4. Free energy profile for the cyclisation pathways depicted in Scheme 7.

Scheme 7. Cyclisation pathways leading from the allylic carbocation intermediate **34**. Bond lengths (Å) shown are for the new bonds formed.
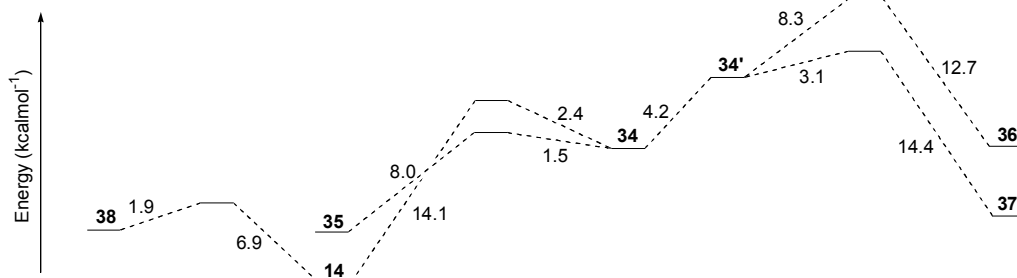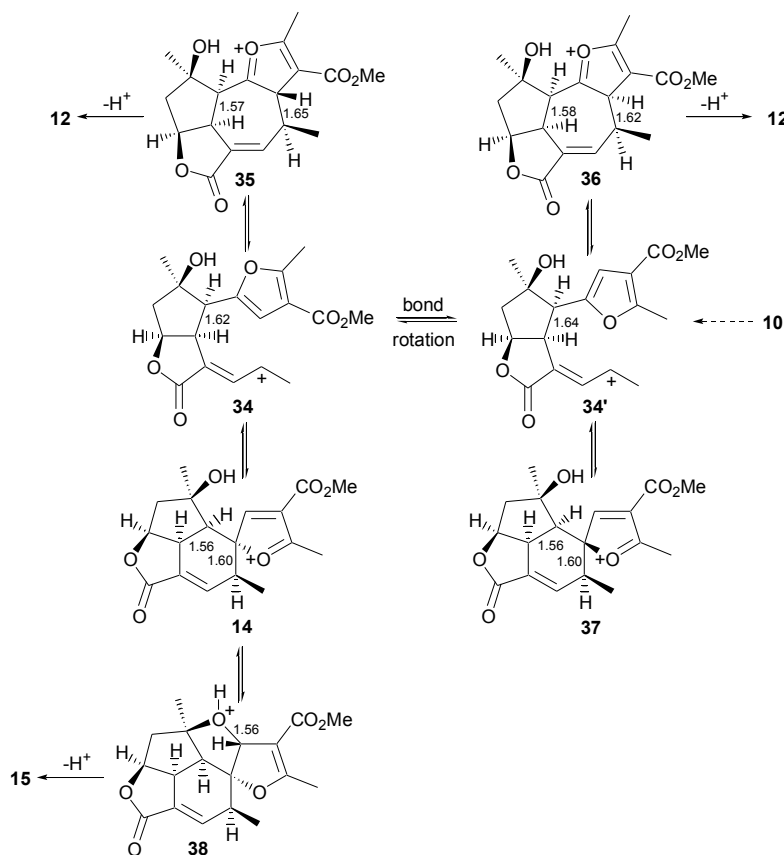
The data presented in Tables 1 and 2 suggest that the stereogenic centre at C8 in the starting isomeric furanoxonium ions **22-25** has a strong influence over the preferred mode of cyclisation. In the C8 α-hydroxy series (R^1=Me, R^2=OH), cyclisation *via* **24** (*Z-exo*) or **25** (*E-endo*) is predicted to be significantly favoured over the alternative pathways. It is notable that these two favoured cyclisation pathways both result in the formation of the same diastereoisomer **27/27'** of the bicyclic intermediate, and that the newly created stereogenic centres match those that result from the *in vitro* acid-promoted cyclisation of the furanobutenolide **16**. In the C8 β-hydroxy series (R^1=OH, R^2=Me), cyclisation *via* the furanoxonium ion

22 (*E-exo*) is predicted to be favoured over the alternatives. This cyclisation would result in the formation of the diastereoisomeric intermediate **26/26'** which, again, is consistent with the outcome of the acid-catalysed cyclisation of the furanobutenolide **10** *in vitro* (Scheme 2).

The origin of these stereoselectivities appears to be largely down to the relative size of the methyl (A-value 1.74 kcal/mol)[17] and hydroxy substituents (A-value 0.61 kcal/mol)[18] at C8 in **10** and **16**, coupled with the requirement for the bulky furyl-fragment to adopt a *pseudo*-equatorial orientation with respect to the forming cyclopentane ring in the first step of the cyclisation. The three most favoured modes of cyclisation are

represented in Figure 2, and each has the larger substituent (CH_3 and furyl) *pseudo*-equatorial and the smaller hydroxyl group *pseudo*-axial. In these structures the forming bonds are

2.14-2.18 Å and the carbon atoms that would complete a (4+2) or (4+3) cycloaddition are 3.29-3.43 Å apart.
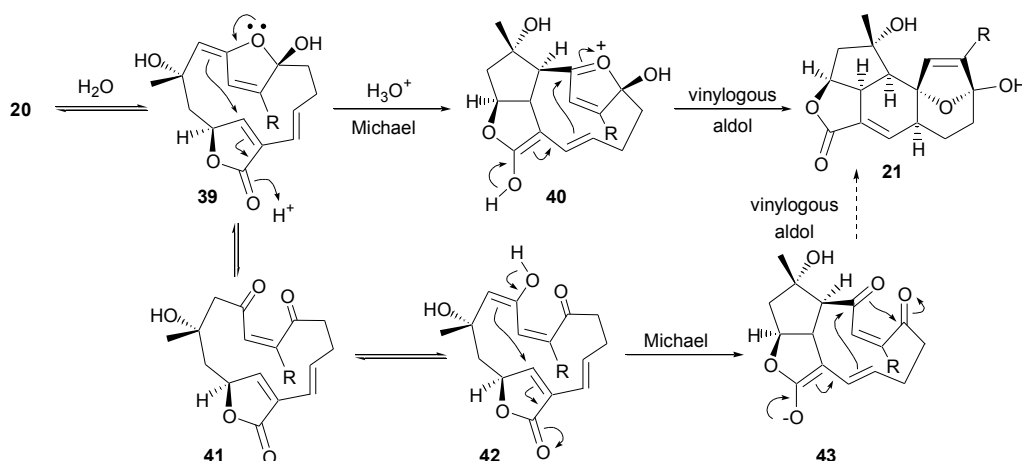
Scheme 8. Alternative transannular cyclisation pathways for the macrocycle **39** to the polycycle **21**.

All the different methods employed for the aforementioned calculations were in qualitative agreement and all suggested the conformational preference of the connecting chain was the main factor determining the stereochemical outcome of the cyclisation. Based on this we concluded that B3LYP/6-31+G(d,p) should be adequate for all subsequent geometry optimisations. We opted to run single-point calculations on optimised geometries using BMK/6-311+G(d,p) to allow comparison with previously published results.[9]

We next considered the possible pathways that could be followed from the carbocation intermediates **26** and **27** to the polycyclic structures **12**, **15** and **17**. The results we obtained for the C8 α-hydroxy series, *i.e.* **16**, are shown in Figure 3 and summarised in Scheme 6. They suggest that the most favourable pathway results in cyclisation to the tetracyclic carbocation **29**. From here, rapid loss of a proton regenerates the furan ring and leads to **17**, the same polycyclic product obtained from the acid-catalysed cyclisation of the furanobutenolide **16** (Scheme 2). Formation of the cyclohexene ring-containing tetracyclic intermediate **32** from **28'** is also predicted to be relatively favourable. However, further cyclisation of **32** to the pentacycle **33** is unfavourable due to the highly strained nature of **33**. This suggests that if the oxonium ion **32** was formed it would either hydrolyse leading to by-products that have not been identified, or simply revert back to the allylic carbocation **28'**.

For the corresponding C8 β-hydroxy series, *i.e.* from **10**, the most favourable pathways that would lead to the products **12** and **15** are shown in Figure 4 and summarised in Scheme 7. It is evident from Figure 4 that very low barrier pathways are predicted for the formation of both of the oxonium ion intermediates **14** and **35**. Furthermore, the cyclisation of **14** leading to the pentacyclic structure **38** is also predicted to be favourable. Loss of a proton from each of the intermediates **35** and **38** would then lead to the same polycycles **12** and **15** that were produced earlier following acid-catalysed rearrangement of the furanobutenolide **10** (Scheme 2).

We next carried out DFT calculations on the cyclisation modes of the macrocycle-based furanoxonium ion **20** and its

corresponding cyclic hemiketal **39** leading to the tetracyclic ring system **21** present in plumarellide **1** (Scheme 8; cf. Scheme 4). Our studies with the acyclic systems **10** and **16** have concluded that their conversions to the polycycles **12/15** and **17** respectively, are more likely to involve stepwise processes *via* carbonium ion intermediates rather than (4+2) cycloaddition reactions. There is also the possibility however that these same cyclisations, and also the cyclisation of the cyclic hemiketal **39** to **21**, could take place by stepwise acid-catalysed cyclisations from the enedione tautomer **41** or from a corresponding enol, *e.g.* **42** of **39**. These new cyclisation possibilities, which are summarised in Scheme 8, were investigated alongside the thermal [4+2] and stepwise carbonium ion cyclisations from **20** and **39** using BMK/6-311+G(d,p)//B3LYP/6-31+G(d,p). The outcomes of these calculations are shown in Figures 5, 6 and 7. As expected, the second step in the stepwise cyclisation of the furanoxonium ion **20** (Figure 5) is predicted to have a higher activation energy than the corresponding acyclic system because it leads to a bridgehead carbonium ion, *i.e.* **44**. The stepwise acid-catalysed pathway **39**→**40**→**21**, shown in Scheme 8 and Figure 6, is predicted to be more favourable than the thermal [4+2] cycloaddition (Figure 7), and the stereochemistry produced in the resulting polycycle is a consequence of the conformation of the macrocycle.

The enedione structure **41** is relatively more stable than its cyclic hemiketal tautomer **39**, which is predicted to be relatively more stable than its enol tautomer **42**, *i.e.* relative energies (kcal/mol) 0 : 7.0 : 9.7.

In contemporaneous studies we synthesised the *Z*-isomer **45** corresponding to **20** and found that when it was treated with TFA in water it underwent cyclisation to the macrocycle **51** in 82% yield, *i.e.* none of the anticipated plumarellide ring system **47** was obtained.[19] The structure **51** is thought to arise *via* an intramolecular [4+2] cycloaddition from the enedione tautomer **48/49** of the hemiketal intermediate **46** (Scheme 9). Clearly the specific aqueous acid conditions we used with **45** drove the equilibrium between **46** and **48** towards the latter. By inference therefore, if we are to realise the conversion of the presumed intermediate **6** into plumarellide *in vitro*, then detailed attention to the nature of any catalyst and reaction conditions will need to

be addressed beforehand to avoid tautomerism to its enedione tautomer leading to unwanted side products. Of course and by contrast, an enzyme mediated cyclisation would not experience the same restrictions on tautomerism and conformational requirements of the substrate **46**.
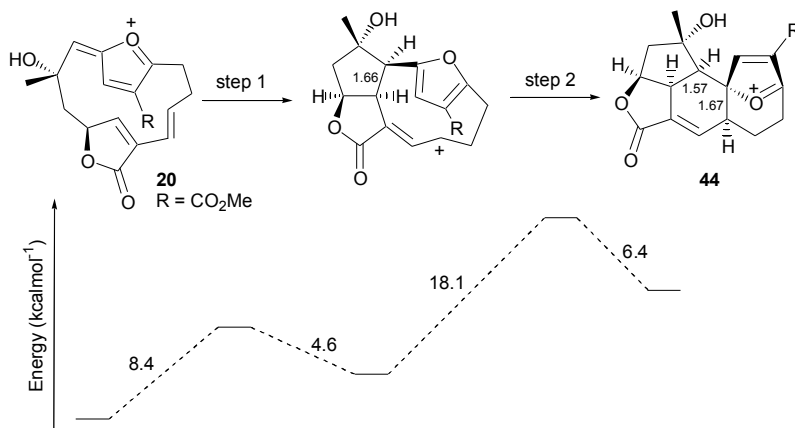

Figure 5. Free energy profile for stepwise cyclisation of the furanoxonium ion **20**. Bond lengths (Å) shown are for the new bonds formed.
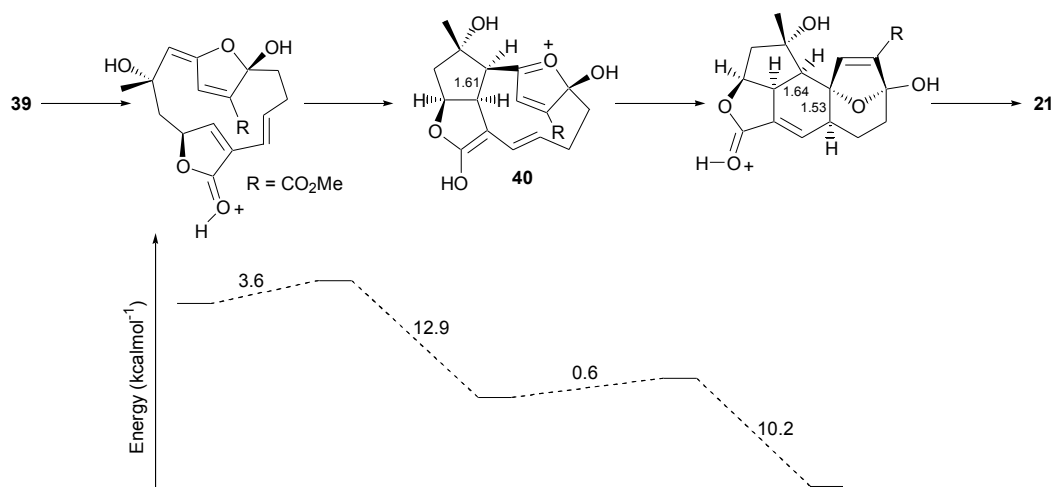

Figure 6. Free energy profile for acid catalysed cyclisation of the cyclic hemiketal **39**. Bond lengths (Å) shown are for the new bonds formed.
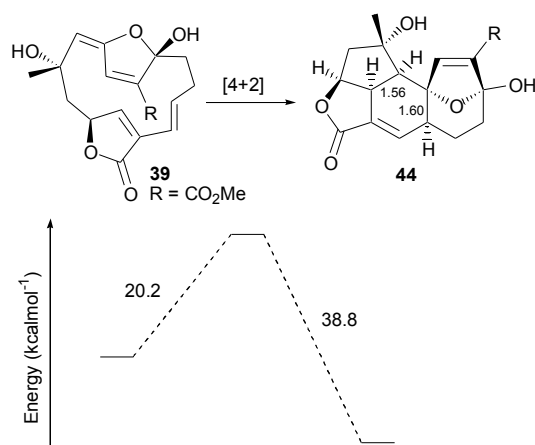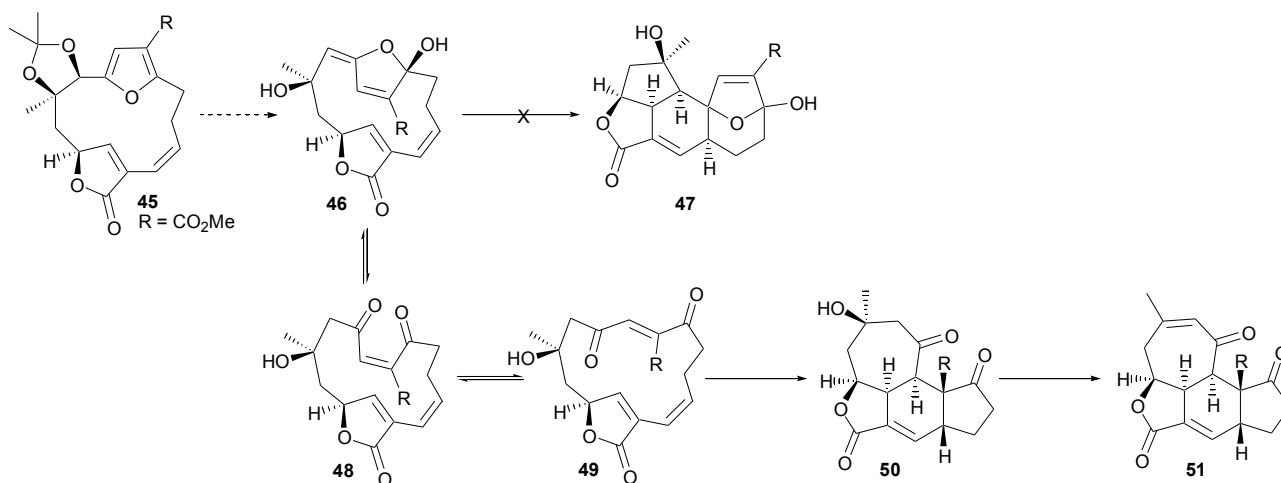

Figure 7. Free energy profile for the concerted [4+2] cycloaddition of the cyclic hemiketal **39**. Bond lengths (Å) shown are for the new bonds formed.

Scheme 9. Formation of the polycycle **51** in preference to the plumarellide ring system **47** from the acid-catalysed rearrangement of the acetonide **45**.

Conclusions

In conclusion, DFT calculations on potential pathways for formation of the tetracycles **12** and **17** and the pentacycle **15** suggest that furanoxonium ion intermediates could be involved. They also predict that stepwise cyclisations would be diastereoselective and favour the products observed. These results are consistent with related studies involving intermolecular reactions between furanoxonium ions and 1,3-dienes, thereby suggesting that the qualitative outcome of related cycloadditions could be predicted using this approach.

Acknowledgements

Notes and references

[a]School of Chemistry, The University of Nottingham, University Park, Nottingham, NG7 2RD, UK

† Electronic Supplementary Information (ESI) available. See DOI: 10.1039/b000000x/

1 Y. Li, G. Pattenden, *Nat. Prod. Rep.*, 2011, **28**, 1269.

2 M. J. Palframan, G. Pattenden, *Tetrahedron Lett.*, 2013, **54**, 324.

3 J. M Winne, G. Pattenden, *Tetrahedron Lett.*, 2009, **50**, 7310.

4 All calculations apart from gCP-D3 corrections were carried out using Gaussian 09 revB.01.[20] Default settings were used except that the UltraFine integration grid was used for calculations involving BMK and M06-2X. Initial structure searches were preformed using B3LYP/6-31G(d),[6] and all resulting structures were further optimized at the B3LYP/6-31+G(d,p) level of theory. Selected structures were also optimized using M06-2X/6-31+G(d,p)[3] in order to confirm that representative geometries had been produced using B3LYP/6-31+G(d,p). BMK/6-311+G(d,p)[4] single-point energies were computed for all B3LYP/6-31+G(d,p) geometries, and combined with B3LYP/6-31+G(d,p) free energy corrections to obtain BMK/6-311+G(d,p)//B3LYP/6-31+G(d,p) free energies. Transition-state structures were all characterized by a single imaginary vibrational frequency, and intrinsic reaction coordinate (IRC) calculations[13] were performed to confirm they connected to the appropriate energy minima. gCP-D3 corrections were applied to B3LYP/6-31G(d) energies using the gCP-D3 Webservice.[7]

5 Estimation of solvation free energies using commonly available PCM methods generally give poor results for flexible polyfunctional charged structures. For recent benchmarking studies see S. Rayne, K. Forest, *Nature Precedings*, 2010 dx.doi.org/10.1038/npre.2010.4864.1; A. V. Marenich, C. J. Cramer, D. G. Truhlar, *J. Phys. Chem. B*, 2009, **113**, 6378; J. P. Guthrie, I. Povar, *Can. J. Chem.*, 2009, **87**, 1154; Y. Takano, K. N. Houk, *J. Chem. Theory Comput.*, 2005, **1**, 70.

6 Lee, C.; Yang, W.; Parr, R. G. *Phys. Rev. B* 1988, **37**, 785; Becke, A. D. *J. Chem. Phys.* 1993, **98**, 1372; Becke, A. D. *J. Chem. Phys.* 1993, **98**, 5648. Stephens, P. J.; Devlin, F. J.; Chabalowski, C. F.; Frisch, M. J. *J. Phys. Chem.* 1994, **98**, 11623.

7 H. Kruse, L. Goerigk, S. Grimme, *J. Org. Chem.*, 2012, **77**, 10824.

8 D. Tantillo, *Nat. Prod. Rep.*, 2013, **30**, 1079; D. Tantillo, *Nat. Prod. Rep.*, 2011, **28**, 1035.

9 J. M. Winne, S. Catak, M. Waroquier, V. Van Speybroeck, *Angew. Int. Ed.*, 2011, **50**, 11990.

10 M. J. Palframan, G. Pattenden, *Synlett*, 2013, 2720.

11 E. M. Krenske, K. N. Houk, M. Harmata, *Org. Lett.*, 2010, **12**, 444.

12 In principle there are four additional cyclisation modes that are possible, but these would lead to a highly strained *trans*-fused bicyclo[3.3.0] ring system.

13 H. P. Hratchian, H. B. Schlegel, *J. Chem. Theory and Comput.*, 2005, **1**, 61

14 Boese, A. D.; Martin, J. M. L. *J. Chem. Phys.* 2004, **121**, 3045.

15 Zhao, Y.; Truhlar, D. G. *Theor. Chem. Acc.* 2008, **120**, 215.

16 For recent discussions on the accuracy of density functionals across a range of applications see, R. Peverati, D. G. Truhlar, *Phil. Trans. R. Soc. A*, 2014, in press; L. Simon, J. M. Goodman, *Org. Biomol. Chem.*, 2011, **9**, 689.

17 H. Booth, J. R. Everett, *J. Chem. Soc., Perkin Trans. II*, 1980, 255.

18 E. L. Eliel, E. C. Gilbert, *J. Am. Chem Soc.*, 1969, **91**, 5487.

19 Y. Li, G. Pattenden, *Tetrahedron Lett.*, 2011**, 52**, 2088.

20 Frisch, M. J.; Trucks, G. W.; Schlegel, H. B.; Scuseria, G. E.; Robb, M. A.; Cheeseman, J. R.; Scalmani, G.; Barone, V.; Mennucci, B.; Petersson, G. A.; Nakatsuji, H.; Caricato, M.; Li, X.; Hratchian, H. P.; Izmaylov, A. F.; Bloino, J.; Zheng, G.; Sonnenberg, J. L.; Hada, M.; Ehara, M.; Toyota, K.; Fukuda, R.; Hasegawa, J.; Ishida, M.; Nakajima, T.; Honda, Y.; Kitao, O.; Nakai, H.; Vreven, T.; Montgomery, J. A., Jr.; Peralta, J. E.; Ogliaro, F.; Bearpark, M.; Heyd, J. J.; Brothers, E.; Kudin, K. N.; Staroverov, V. N.; Kobayashi, R.; Normand, J.; Raghavachari, K.; Rendell, A.; Burant, J. C.; Iyengar, S. S.; Tomasi, J.; Cossi, M.; Rega, N.; Millam, J. M.; Klene, M.; Knox, J. E.; Cross, J. B.; Bakken, V.; Adamo, C.; Jaramillo, J.; Gomperts, R.; Stratmann, R. E.; Yazyev, O.; Austin, A. J.; Cammi, R.; Pomelli, C.; Ochterski, J. W.; Martin, R. L.; Morokuma, K.; Zakrzewski, V. G.; Voth, G. A.; Salvador, P.; Dannenberg, J. J.; Dapprich, S.; Daniels, A. D.; Farkas, Ö.; Foresman, J. B.; Ortiz, J. V.; Cioslowski, J.; Fox, D. J. Gaussian 09, Gaussian, Inc., Wallingford, CT, 2009.